

## Dissipative Soliton Excitability Induced by Spatial Inhomogeneities and Drift

P. Parra-Rivas,<sup>1,2</sup> D. Gomila,<sup>1</sup> M. A. Matías,<sup>1</sup> and P. Colet<sup>1</sup>

<sup>1</sup>*IFISC, Instituto de Física Interdisciplinar y Sistemas Complejos (CSIC-UIB), E-07122 Palma de Mallorca, Spain*

<sup>2</sup>*Applied Physics Research Group (APHY), Vrije Universiteit Brussel, Pleinlaan 2, 1050 Brussels, Belgium*

(Received 10 August 2012; published 5 February 2013)

We show that excitability is generic in systems displaying dissipative solitons when spatial inhomogeneities and drift are present. Thus, dissipative solitons in systems which do not have oscillatory states, such as the prototypical Swift-Hohenberg equation, display oscillations and type I and II excitability when adding inhomogeneities and drift to the system. This rich dynamical behavior arises from the interplay between the pinning to the inhomogeneity and the pulling of the drift. The scenario presented here provides a general theoretical understanding of oscillatory regimes of dissipative solitons reported in semiconductor microresonators. Our results open also the possibility to observe this phenomenon in a wide variety of physical systems.

DOI: [10.1103/PhysRevLett.110.064103](https://doi.org/10.1103/PhysRevLett.110.064103)

PACS numbers: 05.45.Yv, 02.30.Jr, 42.65.Sf, 89.75.Fb

Spatially extended systems display a large variety of emergent behaviors [1], including coherent structures. Particularly interesting is the case of dissipative solitons (DS) [2], exponentially localized structures in dissipative systems driven out of equilibrium, as they can behave like discrete objects in continuous systems. DS can display a variety of dynamical regimes such as periodic oscillations [3–5], chaos [6,7], or excitability [8]. DS emerge from a balance between nonlinearity and spatial coupling, and driving and dissipation. They are unique once the system parameters are fixed, and they are different from the well-known conservative solitons that appear as one-parameter families.

In optical cavities, DS (also known as cavity solitons) have been proposed as bits for all-optical memories [9–13], due to their spatial localization and bistable coexistence with the fundamental solution. In Ref. [8], it was reported that DS may exhibit excitable behavior. A system is said to be excitable if perturbations below a certain threshold decay exponentially, while perturbations above this threshold induce a large response before going back to the resting state. Excitability is found for parameters close to those where a limit cycle disappears [14]. Excitability mediated by DS is different from the well-known dynamics of excitable media, whose behavior stems from the (local) excitability present in the system without spatial degrees of freedom. Excitability of DS is an emergent behavior, arising through the spatial interaction and not present locally. Moreover, the interaction between different excitable DS can be used to build all-optical logical gates [15].

In real systems, however, typically solitons are static, so oscillatory or excitable DS are far from being generic. In this Letter, we present a mechanism that generically induces dynamical regimes, such as oscillations and excitable behavior, in which the structure of the DS is preserved. The mechanism relies on the interplay between spatial inhomogeneities and drift, and therefore, can be implemented

under very general conditions. Inhomogeneities or defects are unavoidable in any experimental setup, and drift is also often present in many optical, fluid, and chemical systems due to misalignments of the mirrors [16,17], nonlinear crystal birefringence [18], or parameter gradients [19], in the first case, and due to the flow of a fluid in the others [20,21]. Roughly speaking, the presence of inhomogeneities and drift introduce two competing effects. On the one hand, an inhomogeneity pins a DS at a fixed position and, on the other, the drift tries to pull it out. If the drift overcomes the pinning, DS solitons are released from the inhomogeneity [19,22]. Thus, depending on the size of the spatial inhomogeneity and the strength of the drift, we observe three main dynamical regimes: (i) stationary (pinned) solutions, (ii) oscillatory regimes, where DS source continuously from the inhomogeneity, and (iii) excitability, where a perturbation may trigger a single DS that is driven away from the inhomogeneity. This scenario does not depend on the details of the system nor on the spatial dimensionality. Besides, it provides a solid theoretical framework to explain the dynamics of DS in systems with drift, as observed, for instance, in semiconductor microresonators [11,22].

To analyze this scenario, we start with the prototypical Swift-Hohenberg equation (SHE), a generic amplitude equation describing pattern formation in a large variety of systems [1,23–25]. The SHE is variational; thus, it cannot have oscillatory regimes. Adding drift and a spatial inhomogeneity we have:

$$\frac{\partial u}{\partial t} = -\left(\frac{\partial^2}{\partial x^2} + k_0^2\right)^2 u + c \frac{\partial u}{\partial x} + r(x)u + au^2 - gu^3 + b(x). \quad (1)$$

Here,  $u(x, t)$  is a real field,  $a$  and  $g$  are real parameters, and  $c$  is the velocity of the drift. The SHE displays DS for  $a > \sqrt{27/38}g$  [24,25], so we take  $a = 1.2$  and  $g = 1$ . We fix

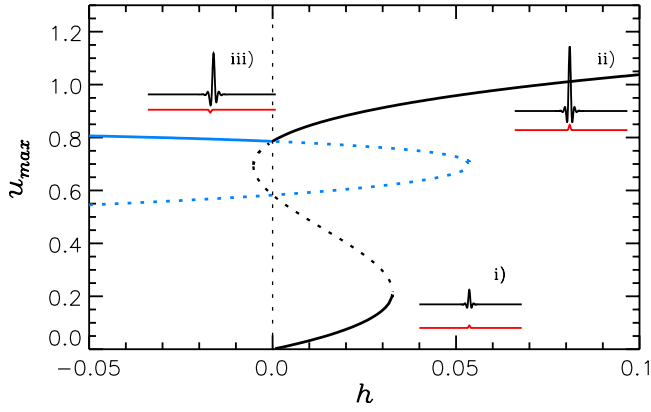


FIG. 1 (color online). Bifurcation diagram showing the maximum of the steady state,  $u_{\max}$ , as a function of  $h$  for  $c = 0$ . In black solutions pinned at their center and in gray (blue) DS pinned at the first tail minima. Solid (dashed) lines indicate stable (unstable) solutions. The insets show the profiles of the solution and the spatial inhomogeneity.

$k_0^2 = 0.5$ . We use a super-Gaussian gain profile  $r(x) = r_0 - 1 + \exp\{-[(x - x_0)/\epsilon]^{18}\}$  to model a finite system of width  $2\epsilon$  so that DS disappear at the boundaries. We fix  $r_0 = -0.2$ , roughly in the middle of the subcritical region where DS exist, and, except where otherwise indicated,  $\epsilon = 94.0842$ . Small changes of the parameter values do not substantially modify the results. A single spatial inhomogeneity located at the center is introduced adding a Gaussian profile  $b(x) = h \exp\{-[(x - x_0)/\sigma]^2\}$  with height  $h$  and half-width  $\sigma$  [26]. This is motivated by the addressing beams used in optical systems to control DS [10,27]. We take  $\sigma = 2.045$ , roughly half the width of a DS. Similar results are found for other values of  $\sigma$  provided the width is small enough to avoid trapping two DS. We have also checked that similar results are found for a defect in the gain profile  $r$ . We take  $h$  and  $c$  as control parameters [28].

For  $c = 0$ , we observe three different steady state solutions which are the main attractors of the dynamics (Fig. 1): (i) the fundamental solution, a low bump corresponding to the deformation of the homogeneous solution, (ii) a high amplitude DS pinned at its center, and (iii) a DS pinned at the first oscillation of its tail. Decreasing  $h$ , at  $h = 0$ , a transcritical bifurcation occurs in which branch (ii) becomes unstable while (iii) is stabilized. Physically, at  $h = 0$  the defect goes from being a bump to a hole. DS tend to sit at the inhomogeneity maximum; thus, a DS centered at the hole becomes unstable and shifts its position until the hole coincides with the first minimum of its tail [29]. At  $h = 0$ , there is also a crossing of unstable middle-branch DS. In what follows, we focus on  $h > 0$ .

This scenario changes when drift is introduced,  $c \neq 0$ : parity symmetry,  $x \leftrightarrow -x$ , is broken making the transcritical bifurcations imperfect. This implies a rearrangement of branches, that for low values of  $c$  leads to the snake-like

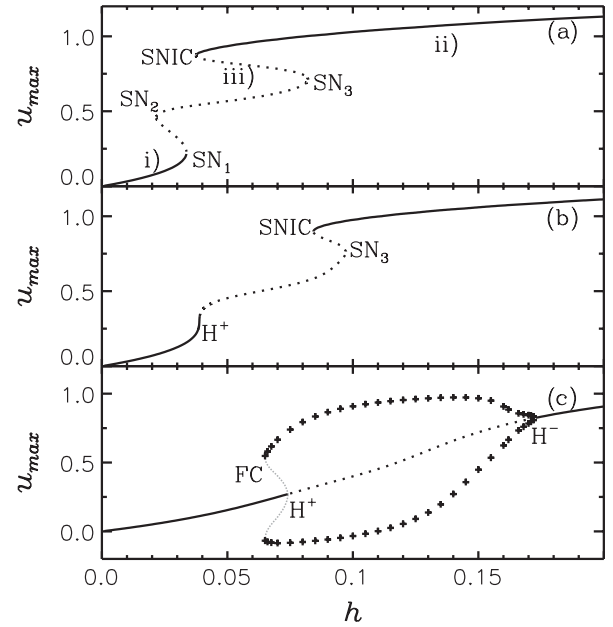


FIG. 2. The same as in Fig. 1 for (a)  $c = 0.05$ , (b)  $c = 0.12$ , and (c)  $c = 0.4$  (see main text). In c) the crosses indicate the maximum and minimum value of the oscillatory DS at a given spatial location. The grey dotted line sketches the maximum and minimum values of the unstable cycle.

branch shown in Fig. 2(a). Saddle-node bifurcations  $SN_1$  and  $SN_3$  where already present for  $c = 0$ . A saddle-node on the invariant circle (SNIC) reconnects branches ii) and iii), while the saddle-node  $SN_2$  arises from the middle branches transcritical bifurcation. Increasing  $c$ , the branch stretches [cf. Fig. 2(b)] and  $SN_1$  coalesces with  $SN_2$  at the cusp bifurcation  $C_1$  as shown in Fig. 3 which displays the general scenario in parameter space. Close to  $C_1$ , there is a Takens-Bogdanov point  $TB_1$  that unfolds a Hopf

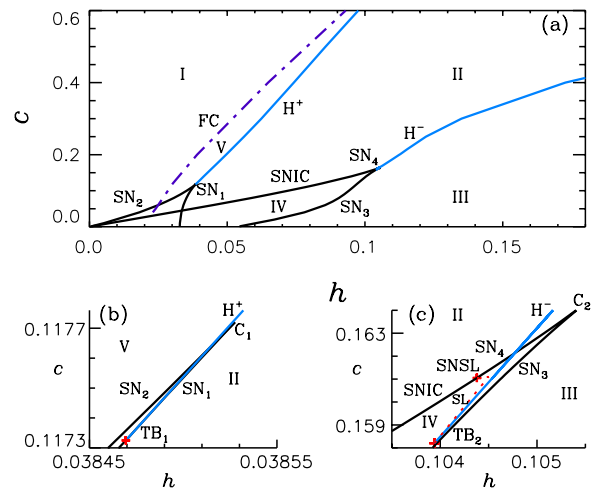


FIG. 3 (color online). (a) Two-parameter ( $c$  vs  $h$ ) phase diagram of the system (see text). Panels (b) and (c) show a zoom close to the cusps and Takens-Bogdanov points.

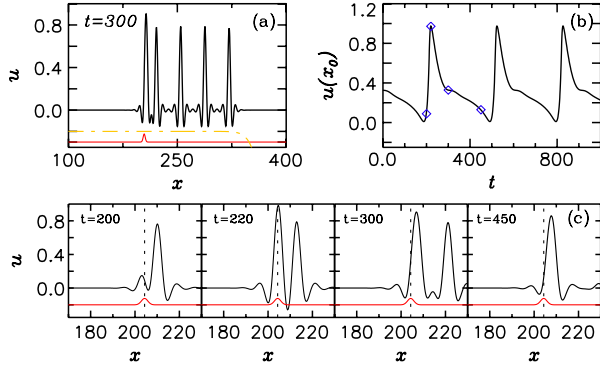


FIG. 4 (color online). (a) Snapshot of a train of solitons in region II of Fig. 3 for  $c = 0.11$  and  $h = 0.076$ . The solid grey (red) and the dot-dashed lines show  $b(x)$  and  $r(x)$ , respectively. Here,  $\epsilon = 163.625$ . (b) Time evolution of the field  $u$  at  $x_0$ . (c) Field profile at the times shown with symbols in (b) showing how a new DS develop and detach.

bifurcation line  $H^+$  [30] [Fig. 3(b)]. As  $c$  keeps increasing, the SNIC line encounters a saddle-node separatrix loop (SNSL) codimension 2 bifurcation from which a saddle-node  $SN_4$  and a saddle-loop SL bifurcation lines unfold [Fig. 3(c)].  $SN_4$  soon coalesces with  $SN_3$  at the cusp  $C_2$  while SL ends at a Takens-Bogdanov point,  $TB_2$ , which also unfolds a Hopf line  $H^-$  tangent to the SL line. Finally, for larger values of  $c$ , there is a single monotonic branch of steady state solutions [Fig. 2(c)]. The Hopf line  $H^+$  is subcritical and is accompanied by a fold of cycles (FC) from which a stable cycle emerges. For  $h$  large enough, the defect is above the threshold to switch on a DS. Thus, this limit cycle corresponds to the periodic creation of DS at the inhomogeneity that are then drifted away [Fig. 4(c)], generating a train of solitons that, in our case, disappear at the boundary of the system [Fig. 4(a)]. Such regime was observed experimentally in semiconductor microresonators [22], where it was called a “soliton tap”. This cycle is stable all the way to the supercritical Hopf  $H^-$ , where  $h$  becomes large enough to prevent the DS being advected by the drift, and the cycle ends.

In parameter space (Fig. 3), the fundamental solution is stable in regions I and V, pinned DS are stable in III and IV, and stable trains of DS exist in II and V. The scenario shown in Figs. 3(b) and 3(c), much richer than in Ref. [8], is characteristic of systems displaying relaxation oscillations described, for instance, by the Van der Pol equation (see Fig. 2.1.2 in Ref. [31]). These systems are characterized by two different time scales, a slow and a fast one. Here, the fast time scale corresponds to the switching time of a DS on the inhomogeneity, while the slow one is the time the drift takes to detach a DS once it is formed [22]. The switch-on time is basically independent on the drift, while the detach time has a strong dependence on it. These two time scales can be clearly identified in a time trace of the field at  $x_0$  [Fig. 4(b)]. Excitability can be found in regions I, III, and IV when applying a perturbation for a

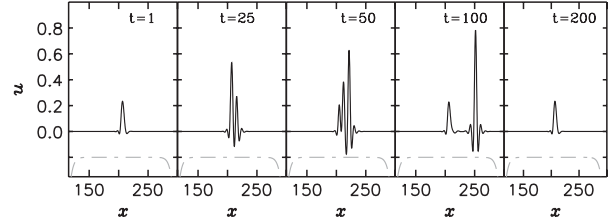


FIG. 5. Excitable excursion of the fundamental solution in region I, close to FC ( $c = 0.6$ ,  $h = 0.085$ ), triggered varying  $h$  an amount  $\Delta h = 0.0325$  during  $\Delta t = 20$  time units. The dot-dashed line shows the gain profile  $r(x)$ .

short time that changes either  $c$  or  $h$ . If the system is brought momentarily into the oscillatory region II then an excitable excursion consisting on the exploration of a loop of the cycle before returning to the original steady state is triggered. An alternative way to trigger an excitable excursion is perturbing the state of the system rather than a parameter [14]. Transient parameter changes are usually easier to implement experimentally; thus, in what follows we consider this kind of perturbations.

In region I, a superthreshold perturbation of the fundamental solution grows to generate a DS, that is then advected away, setting the defect back to the resting state (Fig. 5). As the transition from the stationary state to the oscillatory one is mediated by a subcritical Hopf bifurcation, the excitability is of type II [14]. A clear signature of this type of excitability is that the period of the oscillations remains practically constant as one approaches the threshold from the oscillatory side, namely as one approaches FC coming from region II, as shown in Fig. 6(a). As typical for type II excitability, the threshold is rather a quasi-threshold. If one applies a perturbation that crosses FC but not  $H^+$ , the system will be stacked in region V (bistable). The closer the parameters are to FC, and the closer is FC to  $H^+$ , the smaller is the perturbation required to trigger an excitable excursion [32].

Different dynamics is found in region III, where  $h$  is large enough that, beyond switching on a DS if there is none, it also pins it once it is formed. In this case, DS undergo a supercritical Hopf bifurcation when crossing  $H^-$ . Close to threshold, DS exhibit small oscillations, but decreasing  $h$  or increasing  $c$  just a little further, DS start to source from the inhomogeneity, forming a sort of *canard* in

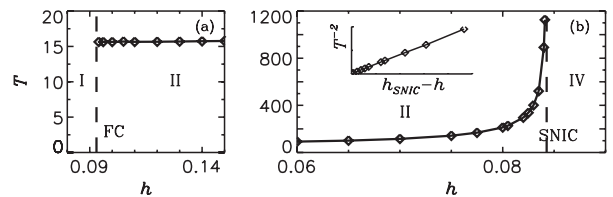


FIG. 6. Oscillation period  $T$  in region II as a function of  $h$  close to a) the FC ( $c = 0.6$ ) and (b) the SNIC ( $c = 0.12$ ). The inset in b) shows the scaling of the divergence of the period.

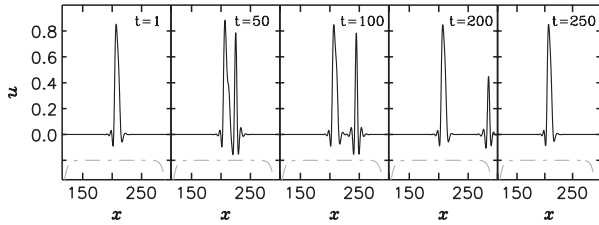


FIG. 7. The same as in Fig. 5 but close to  $H^-$ , in region III. Here,  $c = 0.4$ ,  $h = 0.18$ , and  $\Delta h = -0.045$ .

phase space [33], leading to the train of DS found in region II. This is again a mechanism leading to type II excitability as shown in Fig. 7. At difference with the previous case, here the resting state is a high amplitude DS (see first panel), and the excitable excursion consists of the DS leaving the inhomogeneity and a new one being formed.

There is a third mechanism, associated to the SNIC line separating regions II and IV. A detailed analysis of DS excitability mediated by a SNIC can be found in Ref. [26]. For parameters in region IV, a suprathreshold perturbation that brings the system into region II triggers the unpinning of a DS leading to an excitable excursion. The initial and the final state is a pinned DS and the observed behavior is very similar to the one shown in Fig. 7. In this case, excitability is of type I, whose signature is a divergence of the period. As shown in Fig. 6(b), the period diverges with a power law of exponent  $-1/2$  approaching the SNIC line from region II. A divergence in the period has been reported in semiconductor microresonators [22], induced also through spatial inhomogeneities and drift. Additionally, the SL line in Fig. 3(c) leads to another type I excitable region (discussed at length in Ref. [8]), but at difference with the SNIC bifurcation line, that extends for a wide parameter range, the SL occurs in a very narrow region [Fig. 3(c)], and therefore, it may be more difficult to find experimentally.

In summary, we have shown that the competition between the pinning of DS to a spatial inhomogeneity and the pulling generated by a drift leads to a complex behavior leading to oscillations and to type I and II excitability through several mechanisms. To clearly illustrate this, we make use of the SHE, for which there is a Lyapunov potential [1]; thus, the system always evolves to steady states that minimize the potential. When drift and boundary conditions are added, the SHE no longer has a Lyapunov potential [34]; thus, complex dynamical behavior can arise. In order to confirm the generality of our results, we have checked that the scenario is qualitatively the same in a completely different model displaying DS [35], namely, the Lugiato-Lefever equation [36], which has been recently used to describe DS observed experimentally [12,13]. Our results do not depend on the microscopic details of the system, or the number of spatial dimensions, or the nature of the spatial inhomogeneity, but on general emergent properties of DS, providing a theoretical

framework to explain the dynamics of DS in presence of spatial inhomogeneities and drift in a very broad class of extended systems. The theory presented here gives an explanation to experimental observations [22] and opens up the possibility to observe this phenomenon in a variety of other experimental setups.

Financial support from the MINECO (Spain) and FEDER under Grants No. FIS2007-60327 (FISICOS), No. TEC2009-14101 (DeCoDicA), FIS2012-30634 (INTENSE@COSYP), and TEC2012-36335 (TRIPHOP), from CSIC (Spain) under Grants No. 200450E494 (Grid-CSIC) and No. PIE-201050I016, and from Comunitat Autònoma de les Illes Balears is acknowledged.

- [1] M. C. Cross and P. C. Hohenberg, *Rev. Mod. Phys.* **65**, 851 (1993).
- [2] *Dissipative Solitons*, Lecture Notes in Physics Vol. 661, edited by N. Akhmediev and A. Ankiewicz (Springer, Berlin, 2005); *Dissipative Solitons: From Optics to Biology and Medicine*, Lecture Notes in Physics, Vol. 751 edited by N. Akhmediev and A. Ankiewicz (Springer, Berlin, 2008).
- [3] P. B. Umbanhowar, F. Melo, and H. L. Swinney, *Nature (London)* **382**, 793 (1996).
- [4] W. J. Firth, A. Lord, and A. J. Scroggie, *Phys. Scr.* **T67**, 12 (1996); W. J. Firth, G. K. Harkness, A. Lord, J. McSloy, D. Gomila, and P. Colet, *J. Opt. Soc. Am. B* **19**, 747 (2002).
- [5] V. K. Vanag and I. R. Epstein, *Chaos* **17**, 037110 (2007).
- [6] D. Michaelis, U. Peschel, C. Etrich, and F. Lederer, *IEEE J. Quantum Electron.* **39**, 255 (2003).
- [7] L. Gelens, F. Leo, P. Emplit, M. Haelterman, and S. Coen, *IEEE Photon. Conf. (IPC)*, 364 (2012).
- [8] D. Gomila, M. A. Matías, and P. Colet, *Phys. Rev. Lett.* **94**, 063905 (2005); D. Gomila, A. Jacobo, M. A. Matías, and P. Colet, *Phys. Rev. E* **75**, 026217 (2007).
- [9] W. J. Firth and C. O. Weiss, *Opt. Photonics News* **13**, 54 (2002).
- [10] S. Barland *et al.*, *Nature (London)* **419**, 699 (2002).
- [11] F. Pedaci *et al.*, *Appl. Phys. Lett.* **92**, 011101 (2008).
- [12] F. Leo, S. Coen, P. Kockaert, S.-P. Gorza, P. Emplit, and M. Haelterman, *Nat. Photonics* **4**, 471 (2010).
- [13] V. Odent, M. Taki, and E. Louvergneaux, *New J. Phys.* **13**, 113026 (2011).
- [14] E. M. Izhikevich, *Dynamical Systems in Neuroscience: The Geometry of Excitability and Bursting* (The MIT Press, Cambridge, 2007).
- [15] A. Jacobo, D. Gomila, M. A. Matías, and P. Colet, *New J. Phys.* **14**, 013040 (2012).
- [16] M. Santagiustina, P. Colet, M. San Miguel, and D. Walgraef, *Phys. Rev. Lett.* **79**, 3633 (1997).
- [17] E. Louvergneaux, C. Szwaj, G. Agez, P. Glorieux, and M. Taki, *Phys. Rev. Lett.* **92**, 043901 (2004).
- [18] H. Ward, M. N. Ouarzazi, M. Taki, and P. Glorieux, *Eur. Phys. J. D* **3**, 275 (1998); M. Santagiustina, P. Colet, M. San Miguel, and D. Walgraef, *Opt. Lett.* **23**, 1167 (1998).
- [19] B. Schapers, T. Ackemann, and W. Lange, *IEEE J. Quantum Electron.* **39**, 227 (2003).

- [20] K. L. Babcock, G. Ahlers, and D. S. Cannell, *Phys. Rev. Lett.* **67**, 3388 (1991).
- [21] B. von Haften and G. Izús, *Phys. Rev. E* **67**, 056207 (2003).
- [22] E. Caboche, F. Pedaci, P. Genevet, S. Barland, M. Giudici, J. Tredicce, G. Tissoni, and L. Lugiato, *Phys. Rev. Lett.* **102**, 163901 (2009); E. Caboche, S. Barland, M. Giudici, J. Tredicce, G. Tissoni, and L. Lugiato, *Phys. Rev. A* **80**, 053814 (2009).
- [23] M. Tlidi, P. Mandel, and R. Lefever, *Phys. Rev. Lett.* **73**, 640 (1994).
- [24] P. D. Woods and A. R. Champneys, *Physica (Amsterdam)* **129D**, 147 (1999).
- [25] J. Burke and E. Knobloch, *Chaos* **17**, 037102 (2007).
- [26] A. Jacobo, D. Gomila, M. A. Matías, and P. Colet, *Phys. Rev. A* **78**, 053821 (2008).
- [27] M. Brambilla, L. A. Lugiato, and M. Stefani, *Europhys. Lett.* **34**, 109 (1996); L. Spinelli, G. Tissoni, M. Brambilla, F. Prati, and L. A. Lugiato, *Phys. Rev. A* **58**, 2542 (1998).
- [28] We consider periodic boundary conditions with a system size larger than the gain region. Numerical simulations are performed using a pseudospectral method. Starting from the steady state of a numerical simulation, bifurcation diagrams are found using a Newton method and continuation techniques (see Ref. [8]). Stability is determined from the Jacobian eigenvalues.
- [29] Branch iii) corresponds to pinned DS whose maximum is at the right of the defect. There is also a degenerated branch with the maximum at the left. When the drift is turned-on, the degeneracy is broken. We focus in the DS whose maximum is located downstream, since this branch reconnects to branch ii) when drift is applied.
- [30] L. Gelens, D. Gomila, G. Van der Sande, J. Danckaert, P. Colet, and M. A. Matías, *Phys. Rev. A* **77**, 033841 (2008).
- [31] J. Guckenheimer and P. Holmes, *Nonlinear Oscillations, Dynamical Systems, and Bifurcations of Vector Fields* (Springer, New York, 1983).
- [32] The system is excitable even for  $h = 0$ , although in this case, very large perturbations are required to trigger an excitable excursion.
- [33] K. Bold, C. Edwards, J. Guckenheimer, S. Guharay, K. Hoffman, J. Hubbard, R. Oliva, and W. Weckesser, *SIAM J. Appl. Dyn. Syst.* **2**, 570 (2003).
- [34] C. Cossu and J. M. Chomaz, *Phys. Rev. Lett.* **78**, 4387 (1997).
- [35] D. Gomila, A. J. Scroggie, and W. J. Firth, *Physica (Amsterdam)* **227D**, 70 (2007).
- [36] L. A. Lugiato and R. Lefever, *Phys. Rev. Lett.* **58**, 2209 (1987).